HTML ABSTRACT + LINKS

JOURNAL OF APPLIED PHYSICS VOLUME 96, NUMBER 5 1 SEPTEMBER 2004

Interface instabilities and electronic properties of ZrO_2 on silicon (100)

C. C. Fulton, T. E. Cook, Jr., G. Lucovsky, and R. J. Nemanich
Department of Physics and Department of Materials Science and Engineering, North Carolina State University, Raleigh, North Carolina 27695-8202

(Received 11 March 2004; accepted 4 June 2004)

The interface stability of Zr-based high-*k* dielectrics with an oxide buffer layer was explored with x-ray ($h\nu$=1254 eV) and ultraviolet ($h\nu$=21.2 eV) photoemission spectroscopy. Zirconium oxide films were grown and characterized *in situ* in a stepwise sequence to explore their chemical stability and electronic properties as a function of film thickness and processing conditions. The buffer layers serve to lower the interface state density and to address the high temperature instabilities of ZrO_2 in direct contact with Si. This research addresses three issues: (1) the development of the band offsets and electronic structure during the low temperature ($T<300\,°C$) growth processes, (2) variations in the band structure as effected by process conditions and annealing ($T<700\,°C$), and (3) the interface stability of Zr oxide films at high temperatures ($T>700\,°C$). Annealing the as-grown films to 600 °C results in an ~2 eV shift of the ZrO_2-Si band alignment, giving a band offset that is, favorable to devices, in agreement with predictions and in agreement with other experiments. We propose that the as-grown films contain excess oxygen resulting in a charge transfer from the Si substrate to the internal (ZrO_2-SiO_2) interface and that annealing to 600 °C is sufficient to drive off this oxygen. Further annealing to 900 °C, in the presence of excess Si at the surface, results in decomposition of the oxide to form $ZrSi_2$. *© 2004 American Institute of Physics*.
[DOI: 10.1063/1.1776313]

I. INTRODUCTION

The planned scaling of integrated circuit devices involves a reduction of the gate insulator thickness to obtain the targeted capacitance and sheet charge density in the channel. As the gate dielectric thickness is reduced below 2 nm, direct tunneling between the gate and channel becomes significant, leading to increased power consumption and device failures. As an alternative to reducing the physical thickness of the gate oxide the dielectric constant could be increased. This would allow the desired increase in capacitance with a physically thicker layer, resulting in both a reduced tunneling current and an increase in sheet charge density. With conventional thermal oxides and oxynitrides approaching their physical limits, the exploration of alternative materials has gained significant momentum.[1]

The fundamental criteria for a gate dielectric include band offsets that will block both electrons and holes, chemical stability in contact with both the silicon substrate and the gate material, and a low density of interface electronic states. Zirconium oxides and silicates, with their large band gap of ~5.8 eV and dielectric constants of 15–25, are of particular interest.[1–3] Moreover, the ZrO_2-Si band offsets have been predicted to be favorable for blocking both holes and electrons.[4]

A typical complimentary metal oxide semiconductor process includes a 900–1000 °C dopant activation anneal during which the gate dielectric must not undergo significant chemical changes or interfacial reactions. Previous studies of Zr oxides and silicates on Si have noted several instabilities. The interface between Zr oxides and Si has been reported to be chemically unstable at high temperatures by Chang and Lin, Copel *et al.*, and Stemmer *et al.*, among others.[5–7] Results indicate that the temperature at which the interface decomposes during vacuum annealing is in the range of 880–1000 °C. Chang and Lin noted the instability and suggested possible reaction paths for converting ZrO_2 and $ZrSiO_4$ into gaseous SiO.[5] They have also calculated free energies for these reactions at different temperatures and equilibrium pressures, showing that at low overpressures of SiO and ZrO the decomposition reaction is energetically favorable.

Stemmer *et al.* showed that annealing in an oxygen partial pressure $<10^{-7}$ Torr yielded $ZrSi_2$ precipitates and that greater partial pressures of oxygen can suppress the decomposition reaction.[7] They also found that at high oxygen partial pressures, SiO_2 formation occurs at the dielectric-Si interface.

Other studies have explored the electronic structure of Zr dielectrics on Si. Miyazaki *et al.* found a band gap of 5.5 eV and a valence band offset (VBO) of 3.15 eV for evaporated ZrO_2 on Si(100). Their results also indicated that annealing these films to 500 °C in 10^{-5} Torr dry O_2 does not significantly effect either the band gap or the VBO.[8,9]

In this study, we have spectroscopically explored the chemical and electronic instabilities of Zr oxide on a Si substrate with SiO_2 and Si_3N_4 buffer layers. Using ultrahigh vacuum (UHV) transfer between processing and characterization chambers we were able to perform measurements at various points during film processing and explore the evolution of the Zr oxide films from both a chemical and an electronic perspective.

II. EXPERIMENT

All experiments were performed on 25 mm diameter, *n* type, 0.05 to 1 Ω cm (1×10^{18} to 5×10^{15} cm^{-3} phosphor-

 © 2004 American Institute of Physics

Downloaded 03 Mar 2008 to 152.1.211.43. Redistribution subject to AIP license or copyright; see http://jap.aip.org/jap/copyright.jsp

ous), Si(100) wafers. Prior to loading into UHV the wafers were cleaned with a wet chemical dip in JT Baker 100 for 15 min. at room temperature, a 1 min rinse in deionized water, and a 10:1 HF:H_2O spin etch.

After chemical cleaning the wafer was loaded into a UHV integrated growth and analysis system which includes a linear UHV transfer system interconnecting 13 different process and characterization chambers. Five of these chambers were employed in this study, including plasma oxidation, electron beam deposition of zirconium, solid source molecular beam epitaxy (MBE) deposition of Si, x-ray photoemission spectroscopy (XPS), and ultraviolet photoemission spectroscopy (UPS).

An initial oxygen plasma exposure was employed to remove residual hydrocarbon contamination and to form the thin (0.5 nm) oxide buffer layer. Zirconium oxide thin film growth involved successive steps of zirconium metal deposition followed by plasma oxidation with annealing steps to relax the oxide structure and to explore film stability. After each process step the films were analyzed with XPS and UPS to observe trends in chemical and electronic properties.

The initial O_2 plasma clean/buffer layer formation and subsequent oxidations were performed in a remote plasma-enhanced chemical vapor deposition (RPECVD) chamber with a base pressure of 3×10^{-9} Torr. Plasma exposures took place with a wafer surface temperature of 300 °C, a gas flow of ten standard cubic centimeters per minute (sccm) O_2 and 50 sccm He, and an operating pressure of 60 mTorr He/O_2. Twenty watts of inductively coupled rf power were used to excite the plasma.

Zirconium metal depositions were completed with the substrate at room temperature in a UHV chamber with a base pressure of 5×10^{-10} Torr. The deposited Zr thicknesses of 0.2, 0.4, and 0.8 nm were obtained at rates of 0.04 nm/s where the deposition rate and thickness were measured with a quartz crystal oscillator.

Annealing steps were performed in UHV, with wafers radiatively heated by a coiled tungsten filament and temperatures measured by a thermocouple held behind the center of the wafer. For temperatures of 600 °C and above, the wafer surface temperature was measured with an optical pyrometer; for lower temperatures, the thermocouple reading has been calibrated based on a linear extrapolation from higher temperatures where the pyrometer can be used. A Eurotherm temperature control was employed to regulate the annealing process, utilizing ramp rates of 40 °C/min with maximum sample temperatures held for either 5 or 10 min.

XPS characterization takes place at a pressure of 2×10^{-9} Torr using the 1253.6 eV Mg $K\alpha$ line from a Fisons XR3 dual anode source and a Fisons Clam II electron analyzer. The resolution of the analyzer was determined from the full width half maximum of a gold 4f $_{7/2}$ spectral peak to be ≈1.0 eV; however, through curve fitting, the centroid of spectral peaks can be resolved to ±0.1 eV. Observation "windows" were set around the Si 2*p*, O 1*s*, and Zr 3*d* binding energies to record core level shifts. Ultraviolet photoemission spectra were obtained using a He discharge lamp primarily generating the He I line at 21.2 eV in a chamber with a base pressure of 3×10^{-10} Torr. A VSW 50 mm mean radius hemispherical analyzer and VSW HAC300 were operated with a pass energy of 10 eV resulting in an electron energy resolution of 0.1 eV. A negative 4.00 V bias was applied to overcome the analyzer work function. All photoemission spectra measured binding energy relative to the Si Fermi level and the electron spectrometers have been calibrated with an *in situ* deposited Au film.

The approximate oxide film thickness can be calculated from the thickness of the deposited metal layer using the molar densities and the molar masses of Zr metal and ZrO_2. This analysis gives a ratio of 1.5:1 for the thickness of a ZrO_2 film formed from Zr metal. The estimated film thicknesses discussed here are calculated in this way and assume complete oxidation of the deposited Zr layer. This approach has been corroborated by the relative intensity changes of the Si bulk peak from the Si 2*p* core level spectra, as a function of film thickness.

In addition to the thin (~0.5 nm) SiO_2 buffer layer, separate experiments were conducted where a thick (30 nm) deposited SiO_2 buffer and a 1.0 nm Si_3N_4 buffer were employed to further explore the stability of the Zr oxide. Thick, 30 nm, SiO_2 buffer was deposited by RPECVD using 10 sccm of 1% SiH_4 in He, 10 sccm of O_2, and 50 sccm of He gasses for 120 min. The nitride buffer was formed by exposing a clean Si wafer to an electron cyclotron resonance plasma at 600 °C and 7.5×10^{-4} Torr N_2 for 5 min. After buffer layer formation, ZrO_2 growth proceeds in the same stepwise deposition, annealing, and spectroscopy procedure as was employed with the 0.5 nm SiO_2 buffer. A solid source MBE system was used to deposit 2.0 nm of Si on top of the high-*k* layer to explore stability in the presence of excess Si.

III. RESULTS

A. Low temperature Zr oxide formation

With the stepwise growth and characterization techniques the evolution of the interface chemistry and valence band electronic states can be measured as a function of film thickness. Metal films were deposited in steps of 0.2, 0.2, 0.4, 0.8, and 0.8 nm which, after oxidation, gave cumulative oxide thicknesses of 0.3, 0.6, 1.2, 2.4, and 3.5 nm, respectively, where these values have been determined using the density-ratio approximation discussed above.

In an effort to determine the band bending of the initial oxidized surface we had previously measured the valence band maximum (VBM) and Si 2*p* core level of a clean, hydrogen terminated Si(100) surface.[10] For a wafer of the same specification as those used in this study we find the Si VBM to be 0.85 eV below the Fermi level, and the Si 2*p* core level at 99.65 eV. This gives an energy difference between the Si 2*p* core level and the VBM of $\Delta E=98.8\pm0.1$ eV. The result is similar to that of other reports.[11] The small difference may arise due to the calibrations of the separate electron spectrometers used for our XPS and UPS measurements. The Si 2*p* core level for the initial thin SiO_2 film (observed at 99.65 eV), in conjunction with this ΔE, places the Si fermi level at 0.85±0.1 eV above the VBM. The resistivity range of the substrate also gives the bulk Fermi level at

Downloaded 03 Mar 2008 to 152.1.211.43. Redistribution subject to AIP license or copyright; see http://jap.aip.org/jap/copyright.jsp

TABLE I. Tabulated XPS peak positions and UPS valence band data in binding energy relative to the Si E_F for ZrO_2 deposited on a 0.5 nm SiO_2 buffer layer. The valence band offset (VBO) includes band bending and the conduction band offset (CBO) includes the band gap (9.0 eV for SiO_2 and 5.8 eV for ZrO_2).

Process step	Si 2*p*(*bulk*)	Si 2*p*(SiO_2)	O 1*s*(SiO_2)	O 1*s*(ZrO_2)	Zr 3*d*(*oxide*)	Zr 3*d*(*metallic*)	VBM	BB	VBO	CBO
SiO_2	99.65	103.3	532.5	n/a	n/a	N/a	5.2	0.0	4.3	3.7
0.3 nm	99.45	102.2	531.6	529.9	182.4	N/a	3.4	−0.2	2.3	2.4
0.6 nm	99.45	102.0	531.5	529.7	182.1	N/a	2.7	−0.2	1.6	3.1
1.2 nm	99.40	101.7	531.4	529.5	181.8	N/a	2.2	−0.3	1.1	3.6
2.4 nm	99.40	101.8	531.4	529.4	181.7	N/a	2.1	−0.3	0.9	3.8
3.5 nm	99.30	101.5	531.3	529.1	181.4	N/a	1.9	−0.4	0.7	4.0
600 °C	99.50	103.1	532.5	531.2	183.8	N/a	4.6	−0.2	3.6	1.1
750 °C	99.55	103.3	532.5	531.2	183.7	N/a	4.4	−0.1	3.4	1.3
900 °C	99.45	N/a	N/a	N/a	N/a	179.1	0.0	−0.2	N/a	N/a

$\sim 0.9 \pm 0.1$ eV above the VBM. These results are consistent with flat band conditions after the initial oxidation.

The XPS of the initial plasma oxidized Si(100) surface displayed the bulk Si 2*p* core level at 99.65 eV binding energy and an oxide related peak at 103.3 eV (Table I). These results were essentially identical to our prior report which indicated flat bands at the interface of the SiO_2 buffer layer and the Si.[10] Analysis of the UPS data obtained after the formation of the SiO_2 buffer indicated a VBO of 4.3 eV, in agreement with our previous results and other reports.[10,12]

After the first 0.2 nm Zr deposition and oxidation, the O 1*s* core level spectrum, shown in Fig. 1, indicated a large shift in binding energy. We found that the core level from the as-prepared SiO_2 buffer layer was at 532.5 eV and that after the formation of 0.3 nm of ZrO_2, the strongest peak was then observed at 531.6 eV, with a noticeable shoulder at 529.9 eV. Further growth resulted in the $\sim$529 eV peak becoming more intense, while the peak in the 531 eV range became relatively less intense. Both peaks tended to shift to lower binding energy during the process. At 1.2 nm film thickness, the peaks were of approximately equal intensity and were centered at 531.4 and 529.5 eV, respectively. After the final growth step (3.5 nm film thickness), the more intense peak was at 529.1 eV with a shoulder at 531.3 eV.

The oxide-related Si 2*p* core level, shown in Fig. 2, displayed similar trends, shifting from 103.3 to 102.2 eV after the formation of 0.3 nm ZrO_2. After the deposition of 1.2 and 3.5 nm films, the oxide related Si 2*p* peak was observed at 101.7 and 101.5 eV, respectively. Shifts in the Si 2*p* substrate peak were much smaller, with the peak initially observed at 99.65 eV for the SiO_2 buffer layer, shifting to 99.45 eV for the 0.3 nm film, and finally to 99.30 eV after 3.5 nm had been deposited. We ascribe the shifts in the $\sim$99 eV peak to changes in band bending of the Si substrate.

The Zr 3*d* core level (Fig. 3) displayed an increase in intensity with film thickness, and, like the O 1*s* core level, shifted to lower binding energy with each processing step. The peak position shifted from 182.4 eV for the 0.3 nm Zr oxide to 181.4 eV for the 3.5 nm film.

The UPS spectra of the oxidized films indicated the VBM to be at 3.4 eV binding energy (relative to the bulk Fermi level), after the first 0.3 nm of oxide growth. The VBM shifted progressively toward 1.9 eV with each additional deposition step (Fig. 4). Table I contains a summary of the XPS core level binding energies and the UPS VBM observed during low temperature growth.

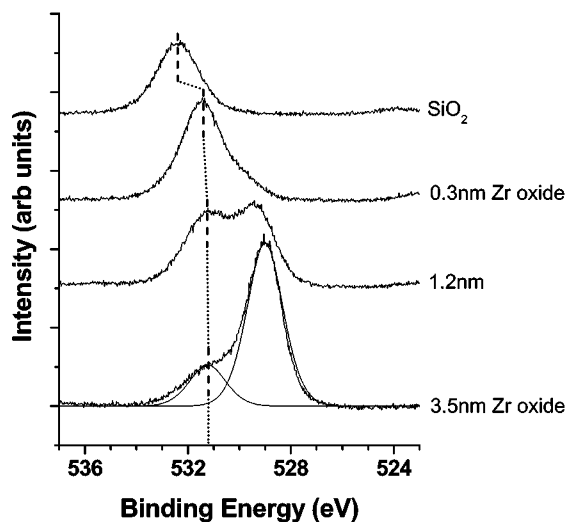

FIG. 1. XPS core level spectra of the O 1*s* transition for various thicknesses of the Zr oxide film on a 1.0 nm SiO_2 buffer layer.

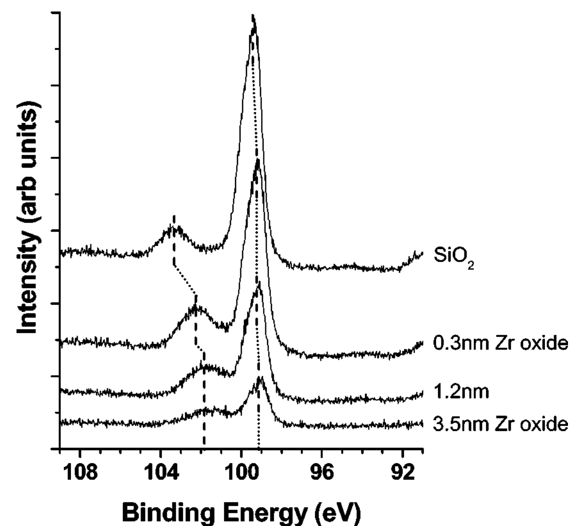

FIG. 2. XPS core level spectra of the Si 2*p* transition for various thicknesses of the Zr oxide film on a 1.0 nm SiO_2 buffer layer.

Downloaded 03 Mar 2008 to 152.1.211.43. Redistribution subject to AIP license or copyright; see http://jap.aip.org/jap/copyright.jsp

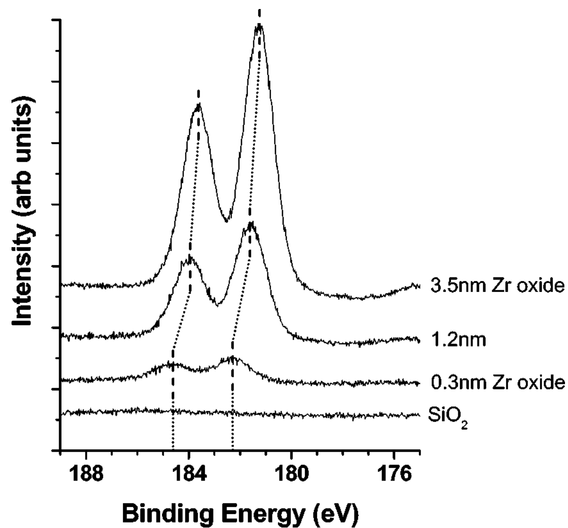

FIG. 3. XPS core level spectra of the Zr 3*d* transition for various thicknesses of the Zr oxide film on a 1.0 nm SiO_2 buffer layer (note the plot order is reversed with respect to Figs. 1 and 2 for clarity).

B. High temperature instability

To explore thermal stability, the stepwise grown film was annealed to 600, 750, and 900 °C. The 600 °C annealing resulted in a large shift in the oxide valence band (Fig. 5), shifting from a binding energy (BE) of 1.9 eV for the as-grown 3.5 nm film to a BE of 4.6 eV for the postannealed film. Further annealing to 750 °C resulted in a 0.2 eV shift of the VBM back toward the Fermi level to a BE of 4.4 eV (Table I).

The core level spectra underwent similar large shifts after annealing to 600 °C (Fig. 6). The O 1*s* spectrum of the as-grown film initially displayed a 529.1 eV peak with a 531.3 eV shoulder, that, after annealing, had shifted to 531.2 eV with a shoulder at 532.5 eV. The Zr 3*d* peak shifted from 181.4 to 183.8 eV. The oxide-related Si 2*p* shifted from 101.5 to 103.1 eV, and the bulk-related Si 2*p* shifted from 99.30 to 99.50 eV. After annealing, the oxide-related Si 2*p* core level showed an increase in intensity and a decrease in peak width compared to the as-deposited state.

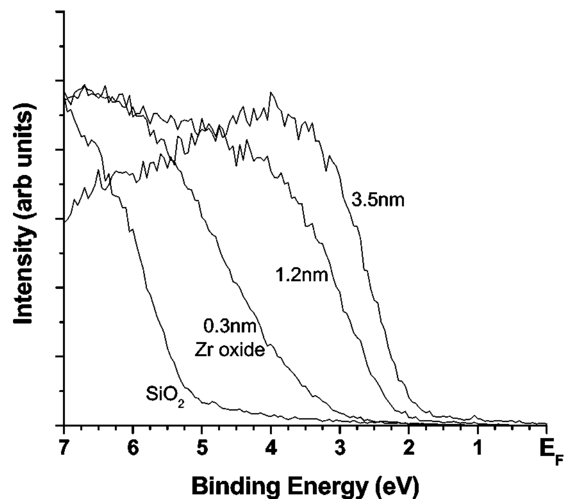

FIG. 4. The UPS valence band spectra for various thicknesses of the Zr oxide film on a 1.0 nm SiO_2 buffer layer.

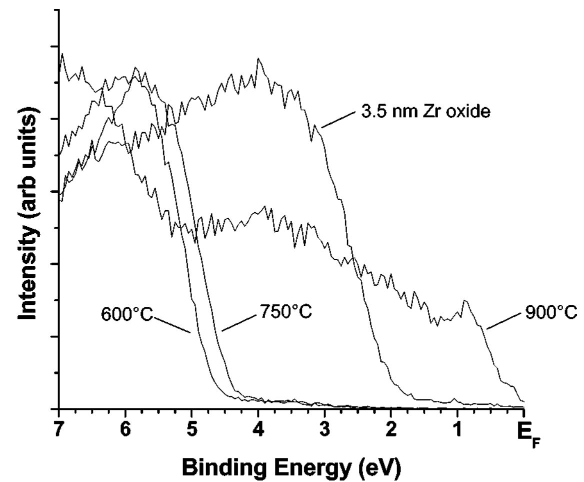

FIG. 5. The UPS valence band spectra for ZrO_2 on a thin SiO_2 buffer layer after different annealing temperatures. The shift from the as-grown 3.5 nm Zr oxide is large (>2 eV) when annealed to 600 °C. There is a smaller shift to lower binding energy as the film is annealed to higher temperature (750 °C). After the 900 °C anneal emission is observed near E_F, indicating the film has a metalliclike character. The relative intensity of each spectrum has been normalized for clarity.

Similar to the changes in the VBM the core level spectra indicated small changes with further annealing to 750 °C. The Zr 3*d* core level was shifted 0.1 eV lower in binding energy, the O 1*s* core levels were unchanged, and the Si 2*p* core levels were both higher in binding energy by 0.2 and 0.05 eV for the oxide- and bulk-related features, respectively.

After annealing to 900 °C the O 1*s* core level was reduced to an almost undetectable level, and the Zr 3*d* peak was shifted to 179.1 eV, a position representative of Zr metal or Zr silicide. The oxide-related Si 2*p* was not observable and the bulk-related Si 2*p* was observed at 99.45 eV, having become much more intense. The UPS spectrum showed emission extending to the Fermi level, indicating a film with a metallic character, and atomic force microscopy (AFM) revealed a high density of islands with radii of ~500 nm.

C. Stability with alternate buffer layers

To explore the conditions of high temperature stability ZrO_2 films were prepared with both a 30 nm SiO_2 buffer layer and a 1 nm Si_3N_4 buffer layer. The 3 nm Zr oxide film was characterized in the as-grown state, annealed, and then characterized again.

After formation of the Zr oxide on the 30 nm SiO_2 buffer, the O 1*s* spectrum displayed peaks at 533.5 and 531.6 eV (Table II). Annealing in UHV to 600 °C resulted in a shift of the 533.5 eV peak to 533.2 eV while the other peak remained unchanged at 531.6 eV (Fig. 7). Annealing to 750 °C found the O 1*s* peaks were at 533.1 eV and 531.5 eV, respectively, and a subsequent 900 °C anneal had shifted them to 533.2 and 531.3 eV. After annealing to 900 °C, the 533.2 eV peak was slightly increased in intensity relative to the peak at 531.3 eV. The oxide-related Si 2*p* core level remained fixed at 104.0 eV through the annealing steps (Fig. 7), and the Zr 3*d* core levels showed small shifts similar to the O 1*s* spectra.

Downloaded 03 Mar 2008 to 152.1.211.43. Redistribution subject to AIP license or copyright; see http://jap.aip.org/jap/copyright.jsp

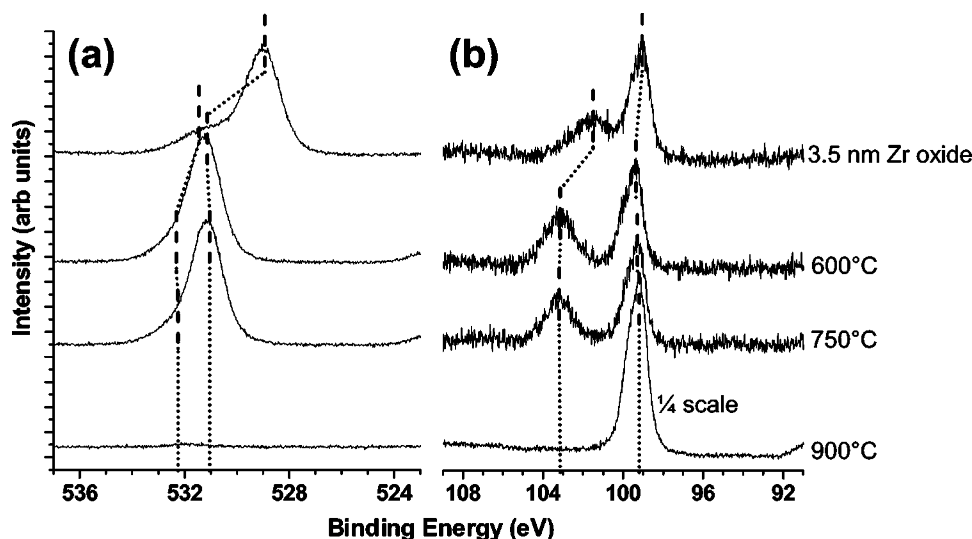

FIG. 6. XPS core level spectra of the (a) O 1*s* and the (b) Si 2*p* transitions for the as-grown 3.5 nm Zr oxide film and after 600, 750 and 900 °C *in situ* anneal. The O 1*s* peak has a large shift when annealed at 600 °C and then disappears after annealing at 900 °C. The oxide related Si 2*p* (~102–103 eV) also shows a sizable shift when annealed to 600 °C and also disappears after annealing to 900 °C. The Si 2*p* bulk peak (~99 eV) becomes much more intense after the 900 °C anneal.

A 2.0 nm thick Si layer was deposited by MBE on the annealed Zr oxide film to explore the effect of excess Si on the decomposition process. After Si deposition the Si 2*p* core level showed a Si bulk peak at 99.55 eV as well as the oxide-related peak at 103.6 eV (Fig. 8). The SiO_2 related O 1*s* peak was unchanged at 533.2 eV, but the ZrO_2 related peak was shifted slightly to 531.5 eV. The Zr 3*d* core level was reduced in intensity due to the Si layer and was shifted to 183.8 eV.

Annealing to 600 °C and subsequently 750 °C (Fig. 8) resulted in a decreased intensity of the Si 2*p* bulk-related core level, and the oxide-related peak shifted back to 104.0 eV. The two peaks of the O 1*s* spectra were at 533.2 and 531.6 eV after both the 600 and 750 °C annealing steps. These peaks also changed in relative intensity with annealing, with the 533.2 eV peak increasing with respect to the 531.6 eV peak.

When annealed to 900 °C the film underwent significant changes. The intensity of the O 1*s* core level was reduced to a level only slightly above the system noise, the oxide-related Si 2*p* core level was not observed, and the Zr 3*d* peak was shifted to a position characteristic of Zr metal or Zr silicide.

To further evaluate the effect of the buffer layer on high temperature stability we deposited a 1 nm Si_3N_4 buffer layer, 3 nm of ZrO_2, and then repeated the annealing experiment, with and without excess Si. The as-grown film as characterized by XPS, displayed core level positions of 99.55 V for the Si 2*p* bulk peak, 101.5 for the Si 2*p* nitride related peak, 529.2 for the O 1*s* peak, and 181.5 eV for the Zr 3*d* core level (Table III). On annealing to 600 °C all of the core level spectra shifted to higher binding energy. The Si 2*p* core levels shifted to 99.70 and 102.3 eV, respectively, the O 1*s* shifted to 530.9, and the Zr 3*d* shifted to 183.2. The films was further annealed to 750 and 900 °C after which the bulk Si 2*p* was observed at 99.80 eV, the nitride bonded Si 2*p* shifted slightly to 102.4 eV, and the O 1*s* and Zr 3*d* were unchanged at 530.9 and 183.2 eV, respectively.

After a 2 nm thick Si layer was deposited via MBE, the bulk Si 2*p* core level was found to be at 99.50 eV, the nitride bonded Si 2*p* was no longer visible, and the O 1*s* and Zr 3*d* core levels had shifted to 531.3 and 183.5 eV, respectively. After annealing to 600 °C the nitride bonded Si 2*p* was once again visible at 102.8 eV, alongside the bulk peak at 99.60 eV. Annealing to 750 °C and finally 900 °C resulted in the emergence of a metallic or silicidelike Zr 3*d* core level at 179.6 eV and a reduction in the oxide-related component at 182.9 eV. After 900 °C the VB spectra was of metallic character, with intensity extending to the Fermi level. The nitride bonded Si 2*p* was detected at 102.2 eV, a position similar to the original Si_3N_4 buffer layer. Tables II and III contain a summary of the data for ZrO_2 films on alternate buffer layers.

TABLE II. Tabulated XPS peak positions and UPS valence band data in binding energy relative to the Si E_F for ZrO_2 deposited on an ~30 nm SiO_2 buffer layer.

Process step	Si 2*p*(*bulk*)	Si 2*p*(SiO_2)	O 1*s*(SiO_2)	O 1*s*(ZrO_2)	Zr 3*d*(*oxide*)	Zr 3*d*(*metallic*)
SiO_2	N/a	104.8	533.9	N/a	N/a	N/a
ZrO_2	N/a	104.3	533.5	531.6	183.9	N/a
600 °C	N/a	104.0	533.2	531.6	183.8	N/a
750 °C	N/a	104.0	533.1	531.5	183.7	N/a
900 °C	N/a	104.0	533.2	531.3	184.0	N/a
Si	95.55	103.6	533.2	531.5	183.8	N/a
600 °C	99.45	104.0	533.2	531.6	184.0	N/a
750 °C	99.60	104.1	533.2	531.6	183.9	N/a
99.55	99.35	N/a	533.5	N/a	N/a	179.2

Downloaded 03 Mar 2008 to 152.1.211.43. Redistribution subject to AIP license or copyright; see http://jap.aip.org/jap/copyright.jsp

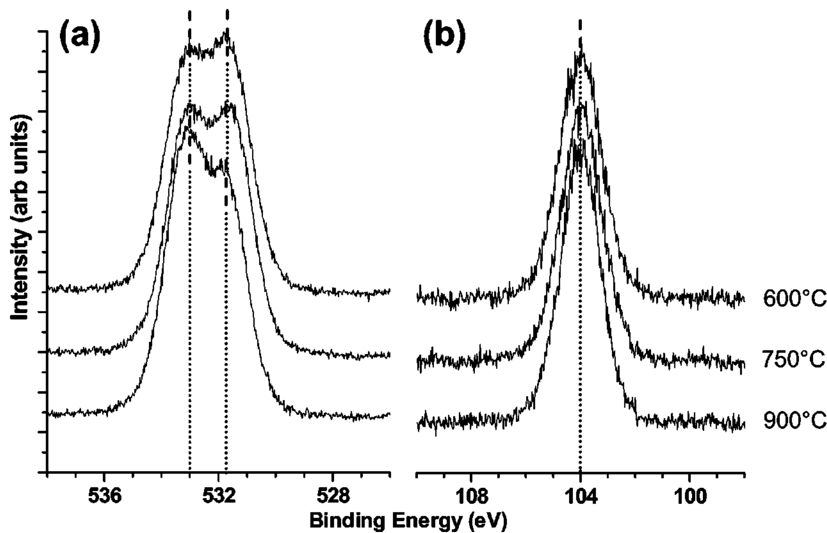

FIG. 7. XPS core level spectra of the (a) O 1*s* and the (b) oxide-related Si 2*p* transitions from 3.0 nm Zr oxide deposited on 30 nm SiO_2.

D. Low temperature instability

The large shifts of the VBM and core levels, observed after annealing to 600 °C, were explored thoroughly in another study that also measured a similar effect observed in Ti and HF oxides.[13] Our observations of ZrO_2 thin films indicated that when annealed at low temperatures, ($T < 600\,°C$) the VBM and core levels shift up to 2 eV. Shifts in the valence band and core levels were observed for annealing temperatures as low as 200 °C. Exposing the annealed film to an oxygen plasma was found to shift the VBM and core levels back to their respective as-grown binding energy positions. Subsequent annealing and oxidation steps consistently shift the band structure and, to within experimental error, give identical results.

These shifts were observed for ZrO_2 deposited on the 0.5 nm SiO_2 and the 1 nm Si_3N_4 buffer layers but not the 30 nm SiO_2 buffer. To explore this, a series of 3 nm ZrO_2 films were deposited on SiO_2 buffer layers of different thicknesses (0.5, 2.0, and 3.5 nm) and the shifts in the electronic structure were measured. Findings from this series of films indicate that the magnitude of the VB and core level shifts decreases with increasing buffer layer thickness, approaching zero as the buffer layer thickness increases beyond 3.5 nm.

IV. DISCUSSION

We divide this section into three parts giving the details of (a) the integrity of the SiO_2 buffer layer during low temperature ZrO_2 deposition, (b) the high temperature instability and oxide decomposition, and (c) the low temperature instability and changes in electronic structure.

A. Integrity of the SiO_2 buffer layer

The relative intensity of the bulk and oxide bonded Si 2*p* core level remained unchanged during film growth, indicating that, to our detection sensitivity, there was no diffusion of Si into the ZrO_2 layer. Nor were any core level shifts observed that would indicate the formation of a Zr silicate. It was also observed that, with annealing to 600 °C, the positions of the Si 2*p* and the SiO_2 related component of the O 1*s* core level return to that of the as-prepared buffer layer. This further suggests that there has been no chemical change of the SiO_2 in the buffer layer. Stemmer *et al.* and Ramanathan *et al.* have shown that the formation of a silicate is thermodynamically unfavorable and that over a wide range of compositions the films will spontaneously phase separate in the amorphous phase.[14–16] Based on this analysis we sug-

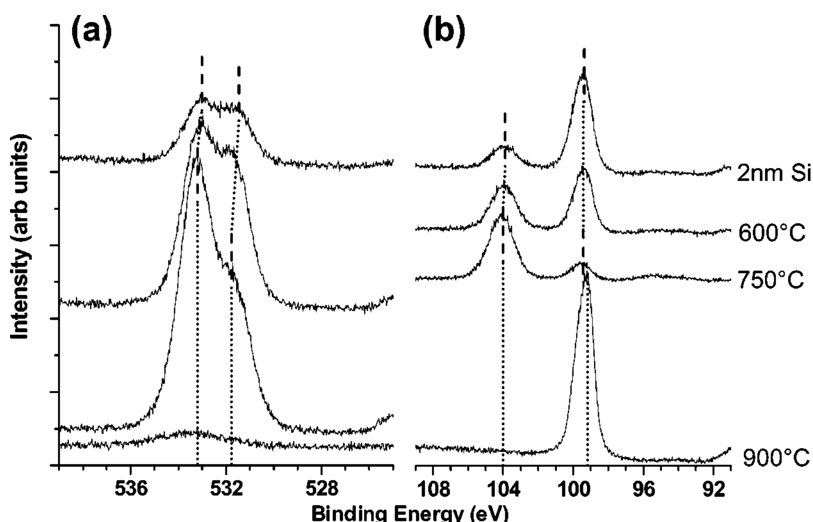

FIG. 8. XPS core level spectra of the (a) O 1*s* and the (b) Si 2*p* transitions from 3.0 nm Zr oxide deposited on 30 nm SiO_2 with a 2 nm Si cap. The oxide-related features are hardly evident after the 900 °C anneal.

Downloaded 03 Mar 2008 to 152.1.211.43. Redistribution subject to AIP license or copyright; see http://jap.aip.org/jap/copyright.jsp

TABLE III. Tabulated XPS peak positions and UPS valence band data in binding energy relative to the Si E_F for ZrO_2 deposited on an ~1 nm Si_3N_4 buffer layer. The valence band offset (VBO) includes band bending. The conduction band offset (CBO) is not given as the band gap values needed to calculate the CBO are not well defined in the presence of excess Si.

Process step	Si 2*p*(bulk)	Si 2*p*(Si_3N_4)	O 1*s*(SiO_2)	O 1*s*(ZrO_2)	Zr 3*d*(*oxide*)	Zr 3*d*(*metallic*)	N 1*s*	BB	VBM	VBO
Si_3N_4	99.75	102.3	532.2	N/a	N/a	N/a	397.8	0.1	N/a	N/a
ZrO_2	99.55	101.5	531.4	529.9	181.5	N/a	397.2	–0.1	2.1	1.1
600 °C	99.70	102.3	N/a	530.9	183.2	N/a	397.6	0.0	4.0	3.1
750 °C	99.85	102.4	N/a	530.9	183.2	N/a	397.8	0.2	4.1	3.3
900 °C	99.80	102.4	N/a	530.9	183.2	N/a	397.5	0.1	4.0	3.2
Si	99.50	n/a	N/a	531.3	183.5	N/a	N/a	–0.2	0.4	N/a
600 °C	99.60	102.8	N/a	531.4	183.6	N/a	397.7	–0.1	3.9	2.9
750 °C	99.65	102.4	N/a	531.2	183.1	179.3	397.5	0.0	2.8	1.9
900 °C	99.65	102.2	N/a	531.9	182.9	179.6	397.6	0.0	0.0	N/a

gest that the low temperature growth process allows us to deposit ZrO_2 on an ultrathin SiO_2 buffer layer while maintaining the integrity of the two layers.

B. High temperature instability

Previous work on Zr oxides has found them to be stable on Si, but only in the limit of temperatures less than ~850 °C.[5,6,17,18] There has, however, been some disagreement about the particular temperature where this instability appears. Copel *et al.* find that 900 °C annealing for 2 min does not lead to decomposition of their ZrO_2 films but that a 30 s flash to 1000 °C does result in decomposition.[6] Chang *et al.* find that 880 °C is sufficient to drive the decomposition reaction at low oxygen partial pressures, and they also propose likely reaction paths, all of which involve excess Si as a reactant (Table IV).[5]

Our results indicate that ZrO_2 films on thin (0.5 nm) SiO_2 buffer layers are unstable at ~900 °C, decomposing into a metallic film, which is most likely $ZrSi_2$. Atomic force microscopy images of the decomposed films display a high density of ~500 nm diameter islands. Stemmer *et al.* have also reported the formation of $ZrSi_2$ islands during vacuum annealing of Zr oxide films on Si.[7]

In contrast to the results for the thin buffer layer, we find that two different buffer layers, a 30 nm SiO_2 layer and a 1 nm Si_3N_4 layer, can both suppress the decomposition reaction during annealing at up to ~900 °C. Moreover, the deposition of a top, 2 nm, Si layer and a second annealing to 900 °C, result in the decomposition of the ZrO_2 film and the formation of Zr silicide. These results indicate that the availability of excess Si leads to the decomposition of the ZrO_2. We suggest that the 0.5 nm SiO_2 layer allows Si to diffuse from the substrate to the high-*k* interface leading to the decomposition reaction. We further suggest that the 30 nm SiO_2 and the 1 nm Si_3N_4 buffer layers inhibit this diffusion and thus prevent the decomposition of the ZrO_2.

Reaction probabilities from a free energy perspective have been calculated by Chang *et al.* and a summary of that work is contained in Table IV.[5] Ramanathan *et al.* have reported that HF and Zr-silicate films tend to phase separate into zirconia and silica during high-temperature anneals, indicating that the first three reaction paths in Table IV are unlikely to occur.[16] Consequently, we expect that the most likely reaction path for the decomposition of our films is the last reaction path given in Table IV, $2ZrO_2+5Si \rightarrow ZrO_{(g)} +3SiO_{(g)}+ZrSi_2$.

Stemmer *et al.* have demonstrated that annealing films in an oxygen ambient rather than in vacuum can improve stability at 900 °C, but these annealing conditions will likely result in SiO_2 growth at the Si interface.[7]

C. Low temperature instability

The large shifts in electronic structure observed with annealing have been explored in another publication, which also includes findings for other transition metal oxides (TiO_2 and HfO_2).[13] The following presents a summary of those results as they apply to ZrO_2.

We suggest that exposure to a remote oxygen plasma (and a high concentration of excited oxygen) introduces excess oxygen into the ZrO_2 film. We further suggest that this excess oxygen is a source of electronic states near the buffer layer—high-*k* interface. Electrons tunnel from the substrate to populate these states, giving rise to a potential across the SiO_2 buffer layer. Annealing removes the excess oxygen and

TABLE IV. Chemical reduction of $ZrSiO_4$ and ZrO_2 involving $SiO_{(g)}$ and $ZrO_{(g)}$ formation. The equilibrium pressures of $SiO_{(g)}$ and $ZrO_{(g)}$ are set at 0.01 Torr at all temperatures, and that $\Delta G_i^o = \Delta G_f^o + RT \ln P_i$ is used for the gaseous species. Values for ΔG are given in kcal/mol for ZrO_2 and $ZrSiO_4$ decomposition.[a]

Reactions	25 °C	527 °C	727 °C	927 °C	1127 °C
$ZrSiO_4+5Si \rightarrow 4SiO+ZrSi_2$	272	141	90	39	−10
$2ZrSiO_4+7Si \rightarrow ZrO+7SiO+ZrSi_2$	620	358	256	155	54
$ZrSiO_4 \rightarrow SiO_2+ZrO_2$	5	4	3	3	2
$SiO_2+Si \rightarrow 2SiO$	130	65	40	15	−9
$2ZrO_2+5Si \rightarrow ZrO+3SiO+ZrSi_2$	349	219	168	118	69

[a]See Ref. 5.

Downloaded 03 Mar 2008 to 152.1.211.43. Redistribution subject to AIP license or copyright; see http://jap.aip.org/jap/copyright.jsp

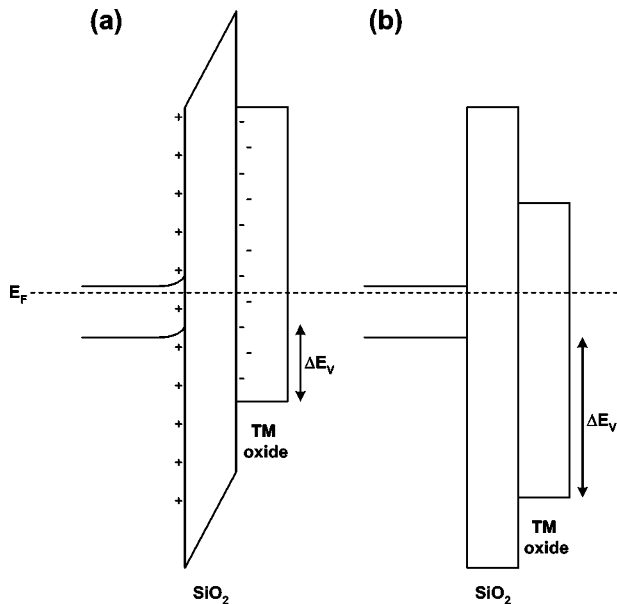

FIG. 9. Schematic diagram of the valence and conduction bands for the (a) as-grown and the (b) annealed state of the TM oxide film on a thin SiO_2 buffer layer. The valence band offset (ΔE_v) can change by up to $\sim$2.5 eV with annealing. The depictions are (a) before *in situ* annealing where excess oxygen near the ZrO_2-SiO_2 interface attracts electrons from the substrate, resulting in a potential across the SiO_2 buffer layer and (b) after *in situ* annealing where the oxygen has diffused to vacuum, reducing the interface electronic states, and the bands become flat.

the associated electronic states, leading to flat bands with no potential across the SiO_2 buffer layer. Figure 9 schematically shows the band structure of the as-grown and annealed ZrO_2 films.

As discussed in Ref. 13, the magnitude of the band structure shift decreases as the buffer layer thickness is increased. With our model, the probability of an electron tunneling through the buffer layer would be expected to decrease as the buffer layer thickness increased. This tunneling dependence would explain the lack of band structure shifts in the ZrO_2 film prepared on a 30 nm SiO_2 buffer layer.

To estimate the charge needed to produce the measured shifts we can treat the buffer layer as a simple dielectric filled capacitor with thickness of $d=1.0$ nm, a dielectric constant of $k=3.9$ for SiO_2, and a voltage of $V=1.0$ V. From this we determine a charge density of $\sim 2\times 10^{13}$ cm^{-2}. We can likewise estimate the positive charge in the Si from the change in band bending at the Si substrate. We use $N_s = \sqrt{2k\varepsilon_0 N_D V/q}$ to calculate the charge density, where N_s is the surface charge density, $N_D = \sim 1\times 10^{18}$ cm^{-3} is the bulk doping density of the Si, q is the charge of an electron, ε_0 is the permittivity of free space, $k=12$ is the dielectric constant of Si, and $V=0.3$ V is the change in band bending. This gives a charge density of $N_s=2\times 10^{12}$ cm^{-2} and, thus, the two calculations are in relative agreement. The excess charge may not be completely localized at the high-k-SiO_2 interface or other conditions may exist to explain the discrepancy in the two different charge density estimates.

Other studies have reported relatively high values of negative fixed charge, $\sim 10^{12}$ cm^{-2}, at internal interfaces between SiO_2 and ZrO_2.[19–21] There have also been reports of positive fixed charge at approximately the same density.[19] Annealing has also been shown to reduce the fixed charge density in films that exhibit either positive or negative fixed charge.[19] The magnitude of the fixed charge density agrees relatively well among the published studies, even for films that have been prepared by different techniques. The sign of the fixed charge, on the other hand, is not well understood, and the conflicting results may suggest that multiple processes are involved. It is evident that further study is needed to correlate processing conditions with the electronic properties of these interfaces.

V. CONCLUSIONS

We have used x-ray and ultraviolet electron spectroscopy to study the chemistry and interface electronic states during the stepwise growth and annealing of ZrO_2 on Si. An interfacial buffer layer of SiO_2 or Si_3N_4 was formed to reduce the number of interface states and improve interface stability. The low temperature deposition technique allowed the formation of ZrO_2 on the buffer layer without mixing, and the two layers remain distinct. Annealing the films to 600 °C resulted in large changes in the band alignment that are attributed to the presence of excess oxygen in the as-grown films. These large shifts of up to 2 eV are consistent and repeatable for multiple oxidation and annealing steps. Annealing at 900 °C resulted in film decomposition into $ZrSi_2$, and a high density of silicide islands was observed with AFM.

The stability of the film at 900 °C was improved by both a thick (30 nm) SiO_2 buffer layer and a 1 nm Si_3N_4 buffer layer. Zirconium oxide films grown on these alternate buffer layers showed little change with annealing at high temperatures. However, a similar 900 °C annealing step after the addition of a 2 nm Si cap led to decomposition of the ZrO_2. These results demonstrate that the presence of excess Si leads to a decomposition reaction of the ZrO_2 thin films and that a thin Si_3N_4 buffer layer may improve thermal stability.

ACKNOWLEDGMENTS

This work was supported through the Semiconductor Research Corporation, the Office of Naval Research, and the Air Force Office of Scientific Research.

[1]G. D. Wilk, R. M. Wallace, and J. M. Anthony, J. Appl. Phys. **89**, 5243 (2001).
[2]J. P. Chang, Y.-S. Lin, S. Burger, A. Kepten, R. Bloom, and S. Levy, J. Vac. Sci. Technol. B **19**, 2137 (2001).
[3]E. P. Gusev, E. Cartier, D. A. Buchanan, M. Gribelyuk, M. Copel, H. Okorn-Schmidt, and C. D'Emic, Microelectron. Eng. **59**, 341 (2001).
[4]J. Robertson, J. Vac. Sci. Technol. B **18**, 1785 (2000).
[5]J. P. Chang and Y.-S. Lin, Appl. Phys. Lett. **23**, 3824 (2001).
[6]M. Copel, M. Gribelyuk, and E. Gusev, Appl. Phys. Lett. **76**, 436 (2000).
[7]S. Stemmer, Z. Chen, R. Kedling, J.-P. Maria, D. Wicaksana, and A. I. Kingon, J. Appl. Phys. **92**, 82 (2002).
[8]S. Miyazaki, M. Narasaki, M. Ogsawara, and M. Hirose, Microelectron. Eng. **59**, 373 (2001).
[9]S. Miyazaki, M. Narasaki, M. Ogasawara, and M. Hirose, Solid-State Electron. **46**, 1679 (2002).
[10]C. Fulton, G. Lucovsky, and R. J. Nemanich, J. Vac. Sci. Technol. B **20**, 1726 (2002).
[11]A. C. Tuan, T. C. Kaspar, T. Droubay, J. W. Rogers, Jr., and S. A. Chambers, Appl. Phys. Lett. **83**, 3734 (2003).
[12]J. W. Kiester, J. E. Rowe, J. I. Kolodziej, H. Niimi, T. E. Madey, and G.

Downloaded 03 Mar 2008 to 152.1.211.43. Redistribution subject to AIP license or copyright; see http://jap.aip.org/jap/copyright.jsp

Lucovsky, J. Vac. Sci. Technol. B **17**, 1831 (1999).
[13]C. C. Fulton, G. Lucovaky, and R. J. Nemanich, Appl. Phys. Lett. **84**, 1 (2003).
[14]S. Stemmer, Z. Q. Chen, C. G. Levi, P. S. Lysaght, B. Foran, J. A. Gisby, and J. R. Taylor, Jpn. J. Appl. Phys., Part 1 **42**, 3593 (2003).
[15]S. Stemmer, Z. Y. Li, B. Foran, P. S. Lysaght, S. K. Streiffer, P. Fuoss, and S. Seifert, Appl. Phys. Lett. **83**, 3141 (2003).
[16]S. Ramanathan, P. C. McIntyre, J. Luning, P. S. Lysaght, Y. Yang, Z. Chen, and S. Stemmer, J. Electrochem. Soc. **150**, F173 (2003).
[17]J.-P. Maria, D. Wicaksanam, A. I. Kingon, B. Busch, H. Schulte, E. Garfunkel, and T. Gustafsson, J. Appl. Phys. **90**, 3476 (2001).
[18]C. M. Perkins, B. B. Triplett, P. C. McIntyre, K. C. Saraswat, and E. Shero, Appl. Phys. Lett. **81**, 1417 (2002).
[19]G. Lucovsky, J. C. Phillips, and M. F. Thorpe, *International Conference on Characterization and Metrology for ULSI Technology* 1998, edited by D. G. Seiler, A. C. Diebold, W. M. Bullis, T. J. Shaffner, R. McDonald and E. J. Walters (The American Institute of Physics,Woodbury, NY 1998), p. 273.
[20]J. P. Chang and Y.-S. Lin, J. Appl. Phys. **90**, 2964 (2001).
[21]J. P. Chang, Y-S. Lin, and C. K. Chu, J. Vac. Sci. Technol. B **19**, 1782 (2001).

Downloaded 03 Mar 2008 to 152.1.211.43. Redistribution subject to AIP license or copyright; see http://jap.aip.org/jap/copyright.jsp